Potential Magnitude of Future Vegetation Change in Eastern North America: Comparisons with the Past

JONATHAN T. OVERPECK, PATRICK J. BARTLEIN, THOMPSON WEBB III

Increases in atmospheric trace gas concentrations could warm the global average temperature 1.5° to 4.5°C by the end of the next century. Application of climate-pollen response surfaces to three climate model simulations of doubled preindustrial atmospheric CO_2 levels shows that the change in the equilibrium distribution of natural vegetation over eastern North America over the next 200 to 500 years could be larger than the overall change during the past 7,000 to 10,000 years and equivalent to the change that took place over the 1,000- to 3,000-year period of most rapid deglaciation. Some plant ranges and abundance maxima could shift as much as 500 to 1000 km during the next 200 to 500 years; such changes would have dramatic impacts on silvicultural and natural ecosystems. Although unprecedented vegetation change is likely if climate changes as predicted, forecasting the exact timing and patterns of change will be difficult.

IN THE CONTEXT OF THE PAST 18,000 years, the climate and vegetation changes of the last two centuries have been small. The next two centuries, by contrast, may experience climatic and vegetational changes unprecedented in the period of the instrumental record. The projected doubling of atmospheric trace gases by the end of the next century may produce a 1.5° to 4.5°C global mean surface warming (*1*). Regional temperature increases, particularly at mid- to high-latitudes, may exceed 10°C and be accompanied by significant shifts in moisture availability (*1, 2*). The sharp contrast between predicted large future change and the small climate changes of the last century indicates that this latter period probably offers an insufficient basis for understanding future climate and vegetation change.

The large climate and vegetation changes of the last 18,000 years provide one context for evaluating possible future changes. Many radiocarbon-dated paleoclimate and pollen records are available for this period. Mean global surface air temperature has increased by approximately 4°C since 18 ka (thousand years ago), primarily in response to changes in the distribution of insolation reaching the earth, the melting of ice sheets, and the warming of sea-surface temperatures (*3*). The magnitude of global temperature change during this period is therefore within the range of that projected for the next century. Future globally averaged warming will likely be more rapid than any time during the past 18,000 years, including during the warming that occurred over the interval of most rapid deglaciation (13 to 9 ka). Major temperature increases primarily in winter but also in summer will likely characterize future climate change, whereas modern temperatures were exceeded in the past primarily in the summer and only by a small amount (*3, 4*). These differences in response, coupled with clear differences between past and future climate forcing, mean that we must rely on models, and not explicit geological analogs, for making realistic assessments of future climate and vegetation change (*5*). Nevertheless, the geological record (i) provides information about the natural variability of the climate system, (ii) shows how vegetation responds to large climatic changes, and (iii) provides a data base against which climate and vegetation models can be tested.

In this paper, we provide a model-based assessment of how the natural vegetation of eastern North America may change over the next two to five centuries in response to trace-gas–induced climate change. We illustrate a simplified scenario in which future climate change stops at the equilibrium state for atmospheric CO_2 levels that are twice preindustrial (A.D. 1750) levels and the vegetation is permitted to adjust to an equilibrium with the changed climate. In reality, the earth's climate is likely to continue warming beyond this equilibrium state (*1*), and vegetation change will probably lag climate change by some amount of time (*6*).

We used pollen data and response surfaces to model the equilibrium response of vegetation to the climate change simulated by atmospheric general circulation models (GCMs). This approach has already been used successfully to simulate modern vegetation patterns (Fig. 1) and the large vegetation changes of the past 18,000 years (*3, 7*). The use of pollen data allows the direct testing of simulated past vegetation change against that observed in mapped abundances of fossil pollen. The relation between pollen and vegetation abundances, although not one-to-one, is approximately linear (*8*). We modeled seven major pollen taxa: sedge (Cyperaceae), spruce (*Picea*), birch (*Betula*), the northern and southern pines (*Pinus*) (*9*), oak (*Quercus*), and prairie forbs (the sum of *Artemisia*, Compositae other than *Ambrosia* and *Iva*, Chenopodiaceae, and Amaranthaceae). These pollen types are representative of the major vegetation regions of eastern North America (Fig. 1): tundra (sedge); boreal forest (spruce, birch, northern pines); mixed conifer-hardwood forest (northern pines and birch); deciduous forest (oak); southern conifer forest (southern pines); and prairie (prairie forbs).

A response surface represents taxon abundances as a nonlinear function of two or more climate predictor variables, and describes how these climate variables jointly control the abundances of a plant taxon. Response surfaces are therefore a type of static vegetation model (*10*). We developed response surfaces for each of the seven pollen types using three climate variables (mean January temperature, mean July temperature, and mean annual precipitation) (*11*). These three climate variables represent the combined general effects of winter temperature stress, summer growing season warmth, and moisture availability on plant abundances. Our results would not be changed significantly by the incorporation of additional predictor variables that are correlated with the three we used. To obtain a range of possible climate scenarios for the effects of doubled CO_2 levels, we used the results from three different atmospheric GCMs (Table 1) (*12*): NASA-GISS, GFDL, and OSU. We coupled each of the seven response surfaces together with both modern observed and simulated future values of mean January temperature, mean July temperature, and annual precipitation to yield estimates of simulated pollen abundances for the present and future (*13*). This approach is identical to that used successfully to model aspects of the observed subcontinental-scale vegetation change of the past 18,000 years (*3, 7, 14*). Comparison of pollen distribution isopoll maps simulated by modern cli-

Table 1. Summary of the three GCM scenarios illustrating the area-averaged change (doubled CO_2 simulation minus control simulation for 1 times CO_2 levels) simulated in our eastern North American study area for the three climate variables used. For more information see (*12*).

Scenario	Mean January temp. (°C)	Mean July temp. (°C)	Mean annual precip. (cm)
GISS	+6.5	+3.0	+5.7
GFDL	+6.8	+6.4	+4.7
OSU	+4.5	+3.4	+6.8

J. T. Overpeck, Paleoclimatology Program, National Geophysical Data Center, National Oceanic and Atmospheric Administration, 325 Broadway, Boulder, CO 80303 and Lamont-Doherty Geological Observatory, Palisades, NY 10964.

P. J. Bartlein, Department of Geography, University of Oregon, Eugene, OR 97403.

T. Webb III, Department of Geological Sciences, Brown University, Providence, RI 02912.

mate data (Fig. 1B) with the actual observed distribution of modern pollen (*15*) (Fig. 1A) illustrates the accuracy of our method.

All three GCM scenarios exhibit broad agreement in the vegetation patterns simulated, and all three suggest that the predicted climate change could lead to significant vegetation change (Fig. 1). Both the ranges and abundance maxima of the taxa we simulated are likely to be displaced northward by at least 100 km and, in some cases (spruce), possibly by as much as 1000 km. The GFDL-based results are the most dramatic because this GCM simulated the greatest summer warming in eastern North America (about 8.5°C maximum warming). The GISS (3.5°C maximum warming) and OSU (3.5°C maximum warming) results also indicate that large-scale shifts in plant ranges could occur when the vegetation reaches equilibrium with these more moderate predictions of future greenhouse climate.

The results for all three models suggest that spruce populations in the eastern United States will decline in abundance, as will populations of northern pines (*Pinus strobus, P. banksiana*, and *P. resinosa*). Even under the GISS and OSU scenarios, the southern range limit of spruce could move northward by as much as 1000 km as high-elevation sites now favorable for spruce at its southern range limit become too warm. Areas now dominated by mixed conifer-hardwood forest could become increasingly deciduous in nature, particularly with large increases in oak abundance in the northern Great Lakes and New England regions. Oak and northern pine populations may move northward by as much as 500 km. Simulated isopoll maps generated with the GISS GCM climate scenario suggest that the northward spread of oak could be further encouraged by local drying in some regions, but the dominance of temperature increases in driving the simulated vegetation change is illustrated by the large shifts induced in the wetter-than-present GFDL and OSU scenarios. A large eastward expansion of prairie forb abundances across the northern United States is simulated by all three GCM scenarios, even in areas where simulated annual precipitation is greater than it is today (that is, in the GFDL and OSU scenarios). The eastward increase in forb percentages suggests that forest biomass could decline even without significant decreases in precipitation. The large simulated eastward expansion of prairie forb populations in the drier-than-present areas of the GISS scenario indicates, however, that regional drying should exacerbate the spread of xeric vegetation at the expense of more mesic vegetation.

In addition to the increase of dry- and warm-adapted prairie taxa across the Great Lakes and northeast regions, the simulated isopoll maps indicate that the northern range boundary of southern pine populations may also expand northward and northeastward by 500 (GISS and OSU) to 1000 (GFDL) km. Birch populations may also be significantly influenced and their areas of greatest abundance could change significantly. Such an effect would change the composition of the Canadian boreal forest. In eastern Canada, the boreal forest may also become more pine-rich than at present. Tundra regions, marked by high abundances of sedge pollen, appear to decline where simulated warming favors the expansion of tree populations.

One way to appreciate the magnitude of the simulated future changes is to compare them with the climate-induced vegetation changes of the past. Isopoll maps are available for the seven taxa (Fig. 1) at 250-year intervals from present to 18,000 years ago (*16*). We used a multivariate dissimilarity measure, the squared chord distance (*17, 18*), to quantify the differences between one set of maps for these taxa (for example, modern observed) and another set of maps either from a date in the past or from one of the model simulations. For each comparison, we calculated squared chord distances at individual grid points (*13*) and then plotted the median and percentiles for the set of squared chord distances from all grid points (Fig. 2). To compare the rates of possible future vegetation change with those that occurred in the past, we also calculated the squared chord distances between sets of maps separated by different intervals of time (500, 1000, and 3000 years).

Our results (Fig. 2A) indicate that the differences between the vegetation distribution for the simulated future climate and present are as large as those between 7 ka (GISS and OSU simulations) or 11 ka (GFDL) and today. The potential change in eastern North American vegetation within

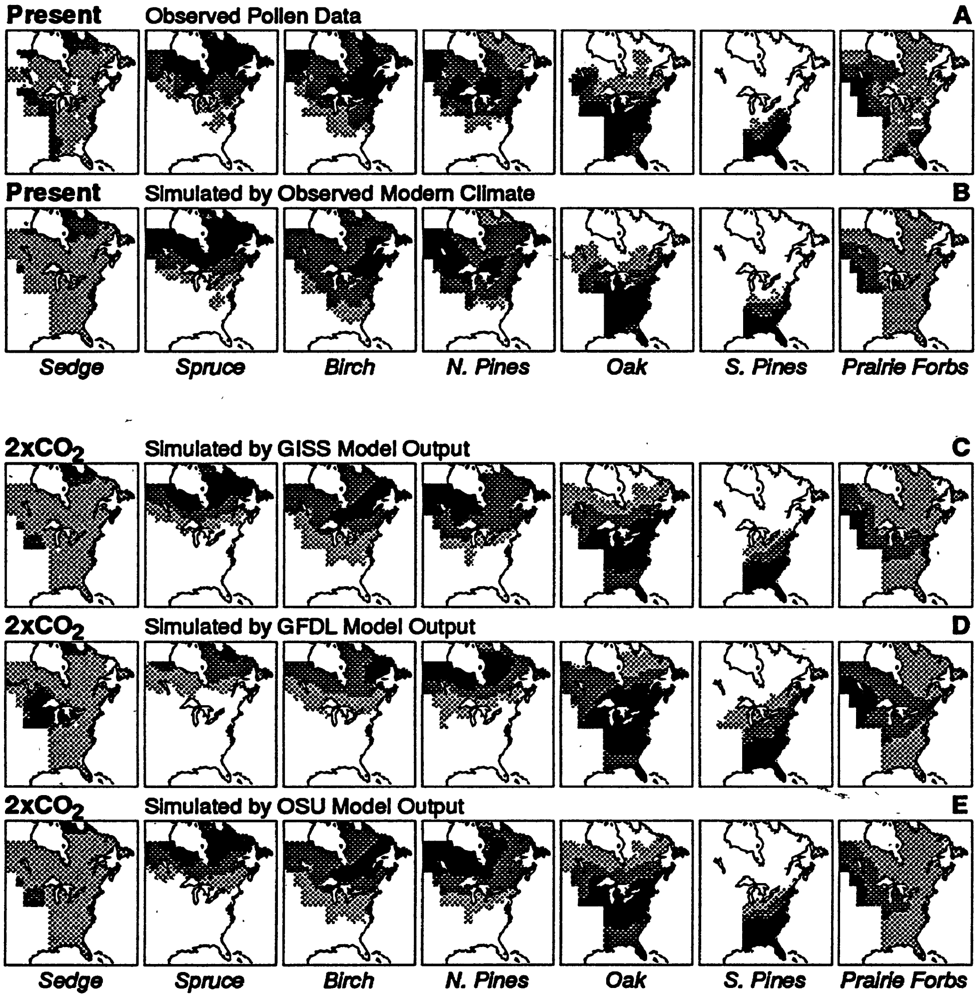

Fig. 1. (**A**) Observed modern pollen abundance; (**B**) equilibrium modern pollen abundances estimated with the use of response surfaces and modern climate data; (**C**, **D**, and **E**) equilibrium pollen abundances estimated by using doubled CO_2 climate scenarios from the three climate models as input to the response surfaces. The shading represents three different levels of abundance: between 0 and 5% (lightest shading), 5 to 20% (medium shading), and greater than 20% (black). The subcontinental patterns observed in modern observed and simulated isopoll maps correspond closely with those in the potential vegetation of the region (*20*).

the next 200 to 500 years therefore may be larger than the total amount of change that took place during the past 10,000 years.

Averaged over eastern North America, the maximum rate of change in the past occurred between 12 and 9 ka during deglaciation (Fig. 2, B to D). This was a period of large-scale vegetational reorganization across eastern North America (*19, 20*). Although some of the changes in pollen distribution that have occurred over 500-year intervals in the past rival the magnitude of changes simulated by the three experiments for doubled CO_2 levels (Fig. 2B), the overall magnitude of the changes simulated by the OSU and GISS models is comparable to the magnitude of the changes that occurred over a 1000-year interval of maximum vegetation change during the last glacial-interglacial transition (Fig. 2C). The GFDL-simulated change is equivalent in magnitude to that which required 3000 years over this transition (Fig. 2D).

Estimating the rates of future climate and vegetation change is not easy (*1*). We do not know the exact rates at which trace gases will be added or removed from the atmosphere. We do not know exactly how much the oceans will act to slow future climate change. We know that the climate models are imperfect in many ways (*1, 2, 21*). These models suggest, however, that transient climate change is likely to reach equilibrium conditions for doubled CO_2 levels sometime near the end of the next century (*1*). In the absence of altered forest disturbance rates, barriers to seed dispersal, or soil limitations, time-dependent vegetation change is also likely to reach the simulated doubled CO_2 patterns (Fig. 1) within 300 to 500 years from now (*14, 22, 23*). Increased rates of forest disturbance may accelerate the rate of vegetation change and lead to the predicted equilibrium vegetation patterns in less than 200 years, but the same change in disturbance rates may also lead to forests that are compositionally and structurally different from those predicted in the absence of disturbance rate increases (*23*). In any case, comparison of the amount of simulated future change to that which occurred in the past (Fig. 2, B to D) suggests that the rate of change during the next 200 to 500 years may exceed the maximum rate of change in the past 18,000 years by two to five times (OSU and GISS) or more (GFDL).

Additional support for our results has been produced with the use of dynamic forest-stand simulation models (*14, 22, 23*) and static (*24*) methods to assess the patterns, magnitudes, and rates of future vegetation change. Results of both response-surface modeling and stand-simulation experiments suggest that elevated temperatures alone may be sufficient to force large-scale vegetation change of the magnitude we have described. Stand-simulation results also corroborate our finding that forest biomass may also increase significantly in some areas and decrease in others (*14, 22*). Our results support paleoecological observations (*18, 20, 25, 26*) that biome compositions will not remain constant as plant taxa respond individualistically to future climate change.

Our assessments are limited to the subcontinental resolution and realism of available GCM scenarios, but they are supported by successful simulations of past climate-induced vegetation change. Assessments of time-dependent change are likely to be much more uncertain than predictions of equilibrium conditions (*1*). Our results indicate that rates of future vegetation change could be extremely high relative to change during the geologic past (Fig. 2) and that assessments of future change could be complicated because natural vegetation of the future may be out of equilibrium with its environment until the rate of climate change is slowed (*24, 27*). Realistic impacts of changing forest disturbance regimes must be included in assessments, along with other important factors, such as soil dynamics, pollution, pests, pathogens, plant migration mechanisms, and direct CO_2 effects (*6, 23, 28, 29*). The exact patterns of future vegetation change may not be predictable for some time, but our results support the possibility that future change may be unprecedented.

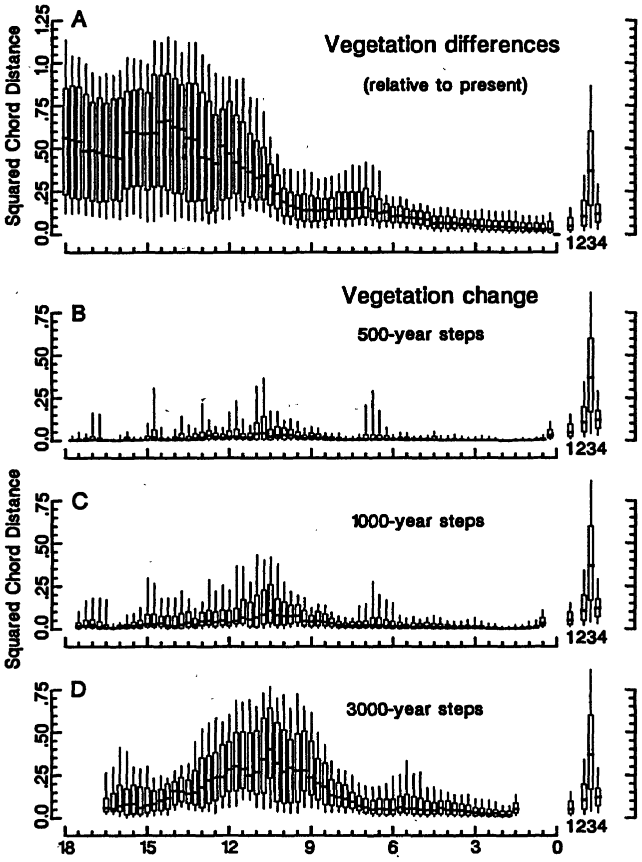

Fig. 2. (**A**) Vegetation differences diagram comparing the potential future vegetation with that of the past 18,000 years. Squared chord distances (*17*) were calculated to measure the differences between: (i) observed modern pollen distributions and those of 250 years ago, 500 years ago, and so on back to 18 ka (from geological data—left graph); (ii) observed modern pollen distributions and the simulated modern distributions (distribution 1 on right); and (iii) the simulated modern pollen distributions and each of the sets of distributions simulated by the experiments for doubled CO_2 levels (distribution 2 for the GISS model, 3 for GFDL, and 4 for OSU on right). The squared chord distances for each comparison are shown as box plots. The center line in each box is the median dissimilarity between two pollen distributions, the edges of the box are the 25th and 75th percentiles, and the lines extend to the 10th and 90th percentiles. Distribution 1 (right) indicates the kinds of dissimilarity that arise from the lack-of-fit of the response surfaces and from the omission of other potentially useful predictor variables. Distributions 2 to 4 show that the differences between the simulated modern maps and those simulated by the experiments for doubled CO_2 levels are large. (**B** to **D**) Vegetation change diagrams showing comparisons between fossil pollen distributions separated by 500 years (B), 1000 years (C), and 3000 years (D) over the last 18,000 years. Fossil sample comparisons are plotted at the midpoint of a sliding window (with a width of 500, 1000, 3000 years) centered on 250-year intervals. For example, the rightmost box on the 500-year time step diagram shows the comparison of 0 years ago with 500 years ago and is plotted at 250 years ago, the next box to the left is for the comparison of 250 and 750 years ago, and so on. Distributions 1 to 4 are repeated for comparison.

REFERENCES AND NOTES

1. J. T. Houghton, G. J. Jenkins, J. J. Ephraums, Eds., *Climate Change: The IPCC Scientific Assessment* (Cambridge Univ. Press, Cambridge, 1990).
2. J. Hansen *et al.*, *J. Geophys. Res.* **93**, 9341 (1988); M. E. Schlesinger and J. F. B. Mitchell, *Rev. Geophys.* **25**, 760 (1987); D. Rind *et al.*, *J. Geophys. Res.* **95**, 9983 (1990).
3. COHMAP Members, *Science* **241**, 1043 (1988).
4. J. E. Kutzbach and P. J. Guetter, *J. Atmos. Sci.* **43**, 1726 (1986).
5. T. Webb III and T. M. L. Wigley, in *Projecting the Climatic Effects of Increasing Carbon Dioxide*, M. C. MacCracken and F. M. Luther, Eds. (Rep. DOE/ER-0237, U.S. Department of Energy, Washington, DC, 1985), pp. 237–258; T. J. Crowley, *J. Clim.* **3**, 1282 (1990); J. F. B. Mitchell, *ibid.*, p. 1177.
6. M. B. Davis, *Clim. Change* **15**, 75 (1989).

7. T. Webb III *et al.*, in *North America and Adjacent Oceans During the Last Glaciation*, W. F. Ruddiman and H. E. Wright, Jr., Eds. (Geological Society of America, Boulder, CO, 1987), pp. 447–462; T. Webb III, *Vegetatio* **69**, 177 (1987).
8. I. C. Prentice, in *Vegetation History*, B. Huntley and T. Webb III, Eds. (Kluwer Academic, Dordrecht, the Netherlands, 1988), pp. 17–42.
9. The split of pines into northern and southern groups was based on the contemporary range maps in E. L. Little, *Atlas of United States Trees*, vol. 1 of *Conifers and Important Hardwoods* (U.S. Department of Agriculture, Washington, DC, 1971). A pollen sum of all tree, shrub, and herb pollen was used to calculate pollen percentages.
10. P. J. Bartlein, I. C. Prentice, T. Webb III, *J. Biogeogr.* **13**, 35 (1986); I. C. Prentice and A. M. Solomon, in *Global Changes of the Past*, R. S. Bradley, Ed. (Office for Interdisciplinary Earth Studies, University Corporation for Atmospheric Research, Boulder, CO, 1991), pp. 365–383; see also (*7*). The latest generation of static models also includes the physiologically based IIASA Biome Model (A. M. Solomon, personal communication).
11. We fit the response surfaces using a three-step procedure: (i) a rectangular grid was generated in the climate space defined by mean January temperature, July temperature, and annual precipitation; (ii) at each grid point, the locally weighted average abundance of a particular pollen type was calculated; and (iii) the surface was depicted by interpolating among those values. Further details may be found in B. Huntley, P. J. Bartlein, I. C. Prentice [*J. Biogeogr.* **16**, 551 (1989)].
12. Output from three different GCMs was used as equilibrium climate for doubled CO_2 levels for eastern North America: (i) the NASA GISS Model II 7.8° latitude by 10.0° longitude GCM [Hansen *et al.*, *Mon. Weather Rev.* **111**, 609 (1983); Hansen *et al.*, in *Climate Processes and Climate Sensitivity*, J. E. Hansen and T. Takahashi, Eds. (American Geophysical Union, Washington, DC, 1984), pp. 130–163]; (ii) the GFDL 4.4° by 7.5° GCM [S. Manabe and R. T. Wetherald, *J. Atmos. Sci.* **44**, 1211 (1987)]; and (iii) the OSU 4.0° by 5.0° GCM [M. Schlesinger and Z. Zhao, "Seasonal climate changes induced by doubled CO_2 as simulated by the OSU atmospheric GCM/mixed layer ocean model" (Oregon State University, Climate Research Institute, 1988)]. Because these models have different sensitivities and regional responses, they provide a useful range of possible future climate scenarios. More detailed descriptions of the scenarios for the three GCMs used are given in J. B. Smith and D. Tirpak, "The potential effects of global climate change on the United States" (Rep. EPA-230-05-89-50, U.S. Environmental Protection Agency, Washington, DC, 1989).
13. Modern (0 ka) control GCM experiments all exhibit systematic biases when compared to observed modern climate (*2, 7*). In order to minimize the potential effects of these biases in our analyses, we applied simulated climate anomalies (experiment with doubled CO_2 levels minus control experiment) to observed modern climate normals (1951 to 1980) for the region.
14. J. T. Overpeck and P. J. Bartlein, in *Rep. EPA-230-05-89-50* (U.S. Environmental Protection Agency, Washington, DC, 1989), chap. 1.
15. To construct the maps of observed pollen data, we used pollen data from 860 samples collected from the surficial (modern) sediments of lakes and mires across eastern North America (*14*) and interpolated these onto a 100-km equal-area grid. The mapped patterns in the observed pollen data reflect the regional vegetation patterns, relatively undisturbed by the effects of settlement by Europeans (*19*).
16. We produced these maps by interpolating the fossil data in (*7*).
17. We first used linear interpolation to assign pollen spectra at each of 243 radiocarbon-dated pollen records (*14*) to time series with a 250-year sampling interval. We then used an inverse-distance weighting method (*7*) to interpolate fossil pollen data for the seven pollen types (Fig. 1) to the same 100-km equal-area grid that was used to interpolate the doubled CO_2 simulations (*13*) and present observed pollen (*15*). We calculated the squared chord distances (d_{ij}) between pairs of pollen spectra (i and j) using:

$$d_{ij} = \Sigma_k(p_{ik}^{1/2} - p_{jk}^{1/2})^2$$

Where p_{ik} is the proportion of pollen type k in pollen spectrum i. The theoretical and empirical advantages of using this dissimilarity coefficient with pollen data are discussed in (*18*).
18. J. T. Overpeck *et al.*, *Quat. Res.* **23**, 87 (1985).
19. G. L. Jacobson, T. Webb III, E. C. Grimm, in *North America and Adjacent Oceans During the Last Glaciation*, W. F. Ruddiman and H. E. Wright, Jr., Eds. (Geological Society of America, Boulder, CO, 1987), pp. 277–288.
20. T. Webb III, in *Vegetation History*, B. Huntley and T. Webb III, Eds. (Kluwer Academic, Dordrecht, the Netherlands, 1988), pp. 385–414.
21. R. D. Cess *et al.*, *Science* **245**, 513 (1989).
22. A. M. Solomon, *Oecologia* **68**, 567 (1986); D. B. Botkin *et al.*, in *Rep. EPA-230-05-89-50* (U.S. Environmental Protection Agency, Washington, DC, 1989), chap. 2.
23. J. T. Overpeck, D. Rind, R. Goldberg, *Nature* **343**, 51 (1990).
24. C. Zabinski and M. B. Davis, in *Rep. EPA-230-05-89-50* (U.S. Environmental Protection Agency, Washington, DC, 1989), chap. 5; W. Emanuel, H. Shugart, M. Stevenson, *Clim. Change* **7**, 457 (1985); D. Lashof, thesis, University of California, Berkeley (1987); K. C. Prentice and I. Y. Fung, *Nature* **346**, 48 (1990).
25. M. B. Davis, *Ann. Mo. Bot. Gard.* **70**, 550 (1983).
26. B. Huntley and T. Webb III, Eds., *Vegetation History* (Kluwer Academic, Dordrecht, the Netherlands, 1988).
27. A. J. Gear and B. Huntley, *Science* **251**, 544 (1991).
28. A. M. Solomon and D. C. West, in *Rep. DOE/ER-0236* (U.S. Department of Energy, Washington, DC, 1985), pp. 145–169; J. Pastor and W. M. Post, *Nature* **334**, 55 (1988).
29. B. R. Strain, *Biogeochemistry* **1**, 219 (1985).
30. This research was supported by a grant from the U.S. Environmental Protection Agency under Interagency Agreement number DW80932629-01 and by the National Science Foundation Climate Dynamics Program. The support of facilities and colleagues at the National Aeronautics and Space Administration Goddard Institute for Space Studies is gratefully acknowledged. We thank R. Goldberg for technical assistance and B. Lipsitz for help with graphics. A. Solomon, J. Cole, E. Cook, L. Donet, G. Jacoby, M. Kneller, and R. Webb provided valuable reviews and discussions of the manuscript. This is Lamont-Doherty Geological Observatory Contribution no. 4838.

11 April 1991; accepted 26 July 1991

Synorogenic Collapse: A Perspective from the Middle Crust, the Proterozoic Grenville Orogen

K. Mezger, B. A. van der Pluijm, E. J. Essene, A. N. Halliday

Structural, petrological, and geochronological studies of the middle to late Proterozoic Grenville orogen in Ontario, Canada, indicate that a major extensional fault developed synchronously with late thrusting. This fault zone was initiated during peak metamorphism and extended into the crust to depths of at least 25 kilometers. The temporal and spatial relations among faulting, metamorphism, and regional compression indicate that synorogenic collapse initiated because the crust exceeded the maximum physiographic height and thickness that could be supported by its rheology. Comparison of Grenville with recent Himalayan orogenic activity suggests that during Proterozoic times physiographic height, crustal thickness, and crustal strength were similar to modern conditions in orogenic belts.

THE DEVELOPMENT OF LARGE-SCALE extensional shear zones and associated rapid thinning of tectonically thickened continental crust is increasingly recognized as a major synorogenic to postorogenic process referred to as "orogenic collapse." Theoretical arguments have been advanced that require extensional tectonics as a consequence of crustal thickening due to compressional tectonics (*1, 2*). Many orogenic belts develop extensional shear zones after the compressional forces cease (*1, 3–5*). Only in a few cases has it been shown that extensional shear zones develop in the upper parts of active orogenic belts while the crust is still undergoing compression (*1, 2*). In this report we provide evidence from the Proterozoic Grenville orogen that synorogenic collapse due to crustal overthickening occurred also in ancient orogenic belts and that collapse structures extended into the middle crust.

The Grenville orogen extends from Labrador to central Mexico and continues on the eastern side of the Atlantic Ocean in Ireland and Scandinavia (*6, 7*). Thus, in extent the Grenville orogen is comparable to the Cordillera of western North America and the Alpine-Himalayan mountain chain. The Grenville orogen is exposed continuously from Labrador to southern Ontario and northern New York. Elsewhere its extent is inferred from small isolated exposures, inliers within younger orogenic belts, xenoliths brought up in young volcanic rocks, drill holes, and geophysical studies [for example (*8, 9*)]. Most of the exposed Grenville orogen is made up of rocks that have experienced at least amphibolite facies metamorphism (550° to 650°C at 6 to 8 kbar), and a large part has undergone granulite facies metamorphism (700° to 800°C at 6 to 11 kbar) [for example (*10*)]. Thus, in

Department of Geological Sciences, C. C. Little Building, The University of Michigan, Ann Arbor, MI 48109.